ISSN 2070-0504, Catalysis in Industry, 2013, Vol. 5, No. 1, pp. 61–73. © Pleiades Publishing, Ltd., 2013.

ENGINEERING PROBLEMS

$MgAl_2O_4$ Spinel Prepared by Mechanochemical Synthesis Used as a Support of Multimetallic Catalysts for Paraffin Dehydrogenation[1]

Sonia A. Bocanegra[a], A. Guerrero-Ruiz[b], Osvaldo A. Scelza[a], and Sergio R. de Miguel[a]

[a] *Instituto de Investigaciones en Catálisis y Petroquímica (INCAPE) , Facultad de Ingeniería Química (Universidad Nacional del Litoral)-CONICET, Santiago del Estero 2654, (3000) Santa Fe, Argentina*

[b] *Departamento de Química Inorgánica y Química Técnica, Facultad de Ciencias, UNED, C/Senda del Rey no. 9, 28040 Madrid, Spain*

e-mail: sbocane@fiq.unl.edu.ar

Received July 6, 2012

Abstract—The catalytic performance in *n*-butane dehydrogenation of bimetallic PtSn, PtGa and PtIn, and trimetallic PtSnIn and PtSnGa catalysts (with low metal contents) supported on a $MgAl_2O_4$ prepared by a novel mechanochemical synthesis was evaluated both in flow and pulse equipment. The influence of the addition of different promoters (Sn, Ga and In) to Pt on the activity, selectivity and deactivation in the *n*-butane dehydrogenation reaction was studied. Stability experiments through successive reaction-regeneration cycles were carried out for selected catalysts. In order to correlate the properties of the metallic phase of the catalysts with the catalytic behavior, several characterization techniques were used, such as test reactions of the metallic phase (cyclohexane dehydrogenation and cyclopentane hydrogenolysis), TPR, XPS, H_2 chemisorption and TEM. Bimetallic PtSn catalyst has a better catalytic behavior than PtIn and PtGa ones. For PtSnM (M: In or Ga) catalysts, whereas Ga addition to the bimetallic catalyst does not practically modify the dehydrogenation performance, the addition of In produces an increase of the activity and the selectivity to butenes. Characterization results indicate the presence of geometric effects for the PtSn catalyst, and geometric and electronic effects for PtIn and PtGa ones. For trimetallic catalysts, the presence of a close contact between Pt, Sn and In or Ga in both trimetallic catalysts was found, mainly due to geometric effects like blocking and dilution of the active sites by the promoters. In stability experiments, the trimetallic PtSnIn/$MgAl_2O_4$ catalyst clearly displays the best catalytic performance along reaction-regeneration cycles, though PtSnGa and PtSn catalysts also showed a very good behavior through the successive cycles. The characterization of these catalysts after cycles shows that their metallic phases are slightly modified along the cycles.

Keywords: paraffin dehydrogenation, $MgAl_2O_4$ support, mechanochemical synthesis, PtSnIn and PtSnGa supported catalysts, characterization of supported catalysts

DOI: 10.1134/S2070050413010030

INTRODUCTION

The most important light olefins used to manufacture different petrochemicals (such as polymers, oxides, alcohols, etc.) are ethylene, propylene and butylenes. The rising demand for these alkenes has exceeded the production capacity of these chemicals by petroleum cracking, the current principal source, thus motivating an interest for seeking other ways of producing them. The catalytic dehydrogenation of ethane, propane, and butane offers an attractive alternative source. In the year 2000, nearly 7 million metric tons of C_3–C_4 olefins were produced via catalytic dehydrogenation [1]. Besides, a further attraction of this process is that hydrogen, the main by-product, is a valuable commodity that can readily be used for many purposes in a petroleum refinery.

The use of a noble metal as a catalytic component, like platinum, leads to an active catalyst for the dehydrogenation of light alkanes, but in the absence of modifiers it has a low selectivity to olefins and a pronounced deactivation due to the rapid coke formation. The addition of inactive metals (like Sn, Ge, In, Ga) to Pt improves the catalytic performance [2–7].

The use of $MgAl_2O_4$ as a catalytic support is based on their neutral acid-base characteristics and very high thermal stability. The first characteristic is very important in paraffin dehydrogenation processes since a very high selectivity to olefins depends not only on the adequate structure of the metallic phase but also on the low acidity of the support in order to minimize the

[1] The article is published in the original.

undesirable lateral reactions (such as cracking and coke formation) [1].

Several articles have been published in the literature reporting the use of $MgAl_2O_4$ synthesized by traditional methods (ceramic and coprecipitation) as catalytic supports for different dehydrogenation reactions [3, 4, 8, 9]. However, there are no studies reporting the use of metallic catalysts (bi and trimetallic ones) supported on Mg spinels prepared by the mechanochemical synthesis in the light alkanes dehydrogenation process. This synthesis method leads to a material with different properties than those synthesized by other techniques (ceramic and coprecipitation ones). This technique improves the contact degree and interaction of the support precursors by the milling process, which increases the chemical homogeneity of the support and reduces the severity of the thermal treatment [10]. In this way, more homogeneous powders can be achieved with similar specific surface areas than the ones obtained by the coprecipitation method [10].

In a previous paper, $MgAl_2O_4$ spinels prepared by different techniques, including the mechanochemical synthesis, were characterized and used as support of monometallic Pt catalysts [11]. In this work, when comparing the $MgAl_2O_4$ synthesized by mechanochemical method with the ceramic one, a material with a higher surface area was obtained, and when comparing with the coprecipitated spinel, a support with a higher metallic dispersion capacity was obtained.

The aim of the present paper is to study the performance of bimetallic PtSn, PtGa and PtIn and trimetallic PtSnIn and PtSnGa catalysts (with low metal contents) supported on $MgAl_2O_4$ prepared by mechanochemical synthesis. Special emphasis was given to the study of the different promoters (Sn, Ga and In) added to Pt, not only on the activity and selectivity, but also on the stability through successive operative cycles (reaction-regeneration-reaction) in the *n*-butane dehydrogenation reaction. Several characterization techniques were used in order to correlate the properties of the catalysts metallic phase with the catalytic behavior in *n*-butane dehydrogenation, such as test reactions of the metallic phase (cyclohexane dehydrogenation and cyclopentane hydrogenolysis), temperature-programmed reduction (TPR), X-ray photoelectron spectroscopy (XPS), H_2 chemisorption, and transmission electron microscopy (TEM).

EXPERIMENTAL

The $MgAl_2O_4$ spinel was prepared by mechanochemical synthesis ($MgAl_2O_4$). Pure MgO (99.9955%) and γ-Al_2O_3 (99.9%) were intimately mixed in 1 : 1 molar ratio and then they were ground to a very fine powder (particle diameter <105 μm) using a mortar. After grinding, distilled water was added to the powder in order to obtain a paste with 45 wt % water content. This paste was milled for 24 h at room temperature by using a ball mill with a cylindrical Teflon body of 140 mL and zirconium balls (13 mm diameter). The milling was carried out with concave rollers at 200 rpm, and the ball/powder weight ratio was 7.5. The paste was dried at 100°C for 12 h, and then submitted to calcination in an electric furnace at 900°C for 12 h in air atmosphere. Finally, the solid was ground to particle sizes between 177 and 500 μm (35–80 mesh).

The BET surface area and the pore volume of the support $MgAl_2O_4$ was obtained by N_2 adsorption at –196°C in a Quantachrome Corporation NOVA-1000 equipment.

X-ray diffraction experiments on $MgAl_2O_4$ were performed at room temperature in a Shimadzu model XD3A instrument using CuK_α radiation (λ = 1.542 Å), generated at 30 kV and a current of 30 mA.

Pt(0.3 wt %)/$MgAl_2O_4$ catalyst was prepared by incipient impregnation of the $MgAl_2O_4$ with an aqueous solution of H_2PtCl_6 at room temperature for 6 h. The Pt concentration in the solution was 2.14 g L^{-1}, and the impregnating volume/weight of support ratio was 1.4 mL g^{-1}. Then the sample was dried at 120°C for 12 h.

Pt(0.3 wt %)Sn(0.3 wt %) bimetallic catalyst was obtained by impregnation of the corresponding monometallic Pt one with an aqueous solution of $SnCl_2$ in diluted hydrochloric acid medium (1 M) at room temperature for 6 h. The concentration of $SnCl_2$ in the impregnating solution was 2.14 g Sn L^{-1}, and the impregnation volume/support weight ratio was 1.4 mL g^{-1}. After impregnation the catalyst was dried at 120°C for 12 h. The Pt(0.3 wt %)Sn(0.3 wt %)In(0.28 wt %)/$MgAl_2O_4$ and Pt(0.3 wt %)Sn(0.3 wt %)Ga(0.17 wt %)/$MgAl_2O_4$ catalysts were obtained by impregnation of the bimetallic one (PtSn) with an aqueous solution (impregnation volume/support weight = 1.4 mL g^{-1}) of $In(NO_3)_3$ or $Ga(NO_3)_3$ at 25°C for 6 h. The In and Ga concentrations (2 g In L^{-1} and 1.21 g Ga L^{-1}) in the impregnating solution were equimolar. Finally, after impregnation, catalysts were dried at 120°C overnight and calcined in air at 500°C for 3 h.

Two different *n*-butane dehydrogenation tests were carried out, one of them in a continuous flow reactor and the other one in a pulse equipment. The continuous flow experiments were performed at 530°C for 2 h in a quartz flow reactor heated by an electric furnace. In this case, the reactor (with a catalyst weight of 0.200 g) was fed with 18 mL min^{-1} of the reactive mixture (*n*-butane + hydrogen, H_2/n-C_4H_{10} molar ratio = 1.25). The reactive mixture was prepared in situ by using mass flow controllers. All gases, *n*-butane, N_2 (used for purge), and H_2 (used for the previous reduction of catalysts and for the reaction) were high purity ones (>99.99%). Prior to the reaction, catalysts were

reduced in situ at 530°C under flowing H_2 for 3 h. The reactor effluent was analyzed in a GC-FID equipment with a packed column (1/8 × 6 m, 20 wt % BMEA on Chromosorb P-AW 60/80), which was kept at 50°C during the analysis. With this analytical device, the amounts of methane, ethane, ethylene, propane, propylene, *n*-butane, 1-butene, *cis*-2-butene, *trans*-2-butene and 1,3 butadiene were measured. The *n*-butane conversion was calculated as the sum of the percentages of the chromatographic areas of all the reaction products (except H_2) corrected by the corresponding response factor. The selectivity to the different reaction products (*i*) was defined as the ratio: mol of product i/Σ mol of all products (except H_2). Taking into account the high temperatures used for the reaction (for thermodynamic reasons), it was necessary to determine the contribution of the homogeneous reaction. For this purpose, a blank experiment was performed by using a quartz bed and the results showed a negligible *n*-butane conversion ($\ll$1%).

The pulse experiments were performed by injecting pulses of pure *n*-butane (0.5 mL STP) into the catalytic bed (0.100 g of sample) at 530°C. The catalytic bed was kept under flowing He (30 mL min^{-1}) between the injections of two successive pulses. Prior to the experiments, all samples were reduced in situ under flowing H_2 at 530°C for 3 h. The composition of each pulse after the reaction was determined by using a GC-FID equipment with a packed column (Porapak Q). The temperature of the chromatographic column was 30°C. In these experiments the *n*-butane conversion was calculated as the difference between the chromatographic area of pure *n*-butane fed to the reactor and the chromatographic area of non-reacted *n*-butane at the outlet of the reactor, and this difference was referred to the chromatographic area of *n*-butane fed to the reactor. The selectivity to a given product was calculated in the same way than for flow experiments. The carbon amount retained on the catalyst after the injection of each pulse was calculated through a mass balance between the total carbon amount fed to the reactor and the total carbon amount detected by the chromatographic analysis at outlet of the reactor. The accumulative carbon retention was calculated as the sum of the carbon amount retained after each pulse.

Besides the above mentioned test in *n*-butane dehydrogenation, the catalytic stability of the bimetallic PtSn(0.3 wt %)/$MgAl_2O_4$ and PtSn(0.3 wt %)/$MgAl_2O_4$ catalysts was also studied. The stability experiments consisted on five reaction-regeneration cycles. Each sequence was: reaction (at 530°C, 6 h), purge with N_2, regeneration with a O_2–N_2 mixture (5% v/v O_2) at 500°C for 6 h, purge with N_2 and reduction with H_2 at 530°C for 3 h. The purge steps with N_2 were performed at 400°C for 30 min. The catalyst weight (0.500 g) used in these experiments was higher than that of the flow experiments in order to magnify the thermal effects during reaction, regeneration (carbon burn-off, a very exothermic reaction) and reduction (an exothermic reaction) steps.

Test reactions of the metallic phase, cyclohexane dehydrogenation (CHD) and cyclopentane hydrogenolysis (CPH), were carried out in a differential flow reactor with volumetric flow of 6 cm^3 h^{-1}. Prior to these reactions, samples were reduced in situ with H_2 at 500°C for 3 h. In both reactions the H_2/hydrocarbon molar ratio was 26. The reaction temperatures in CHD and CPH were 300°C and 500°C, respectively. The activation energy in CHD for different catalysts was obtained by measuring the initial reaction rate at 270, 285 and 300°C. The sample weight was chosen so that the conversion was lower than 7%. Deactivation of the samples was not observed during the experiments.

TPR experiments were performed in a quartz flow reactor. The samples (fresh and after five reaction-regeneration cycles) were heated at 6°C min^{-1} from room temperature up to about 600°C. The reductive mixture (5 v/v % H_2–N_2) was fed to the reactor with a flow rate of 10 mL min^{-1}. Catalysts were previously calcined "in situ" at 500°C for 3 h.

XPS measurements were carried out in a VG-Microtech Multilab spectrometer, which operates with an energy power of 50 eV (radiation MgK_α, $h\nu = 1253.6$ eV). The pressure of the analysis chamber was kept at 4×10^{-10} torr. Samples were previously reduced in situ at 500°C with H_2 for 2 h. Binding energies (BE) were referred to the C1s peak at 284.9 eV. The peak areas were estimated by fitting the experimental results with Lorentzian–Gaussian curves.

H_2 chemisorption measurements were made in a volumetric equipment. The sample was heated under flowing H_2 (60 mL min^{-1}) from room temperature up to 500°C, and then kept at this temperature for 4 h. Then, the sample was outgassed under vacuum (10^{-4} torr) for 1 h. After the sample was cooled down to room temperature (25°C), the hydrogen dosage was performed in the range of 50–250 torr. The chemisorbed hydrogen was calculated by extrapolation of the isotherms to pressure zero.

TEM measurements were carried out on a JEOL 100CX microscope with a nominal resolution of 0.6 nm, operated with an acceleration voltage of 100 kV, and magnification ranges of 80000× and 100000×. The samples (fresh and after five reaction-regeneration cycles) were prepared by grinding, suspending and sonicating them in ethanol, and putting a drop of the suspension on a carbon copper grid. After evaporation of the solvent, the specimens were introduced into the microscope column. For each catalyst, a very important number of Pt particles were observed and the distribution curves of particle sizes were done. The mean metallic particle diameter (*D*) was calculated as: $D = \frac{\Sigma n_i d_i}{\Sigma n_i}$, where n_i is the number of particles of diameter d_i.

Table 1. Results of H_2 chemisorption, inicial rates (R_{CH}) and activation energies (E_{CH}) in CH dehydrogenation, and initial rates (R_{CP}) in CP hydrogenolysis for Pt, PtSn, PtSnIn and PtSnGa supported on $MgAl_2O_4$

Catalyst	H_2 chemisorption (μmol g cat.$^{-1}$)	CH dehydrogenation		CP hydrogenol.
		R°_{CH}, mol h^{-1}g^{-1}	E_{CH}, kcal mol^{-1}	R°_{CH}, mol h^{-1}g^{-1}
$Pt/MgAl_2O_4$	3.82	101.8	21.0	4.7
$PtSn(0.3)/MgAl_2O_4$	1.10	49.7	18.7	1.9
$PtIn(0.28)/MgAl_2O_4$	2.33	18.4	34.9	1.3
$PtGa(0.17)/MgAl_2O_4$	2.66	16.7	41.1	1.2
$PtSn(0.3)Ga(0.17)/MgAl_2O_4$	<0.05	<3	–	0.9
$PtSn(0.3)In(0.28)/MgAl_2O_4$	<0.05	<3	–	0.7

Note: n.d.: no detected.

RESULTS AND DISCUSSION

Characterization of the Support

The values of S_{BET} and pore volume were 117 $m^2 g^{-1}$ and 0.38 $cm^3 g^{-1}$, respectively. The high value of the specific surface area obtained by the mechanochemical method in comparison with those obtained by other techniques [10] should be noted.

Influence of Sn, Ga and In Added to $Pt/MgAl_2O_4$ Catalyst

The results of both test reactions (CHD and CPH) are shown in Table 1. It is observed that the addition of the second metal (Sn, In or Ga) to Pt causes a decrease of R_{CH} values. This fall is more marked for PtGa and PtIn catalysts (R°_{CH} of these bimetallic catalysts is about five times lower than that of the Pt catalyst). For the PtSn catalyst, R°_{CH} is half that of the Pt catalyst. With respect to the values of activation energy (E_{CH}), the PtSn catalyst shows a similar value to that of the Pt catalyst, whereas those of PtGa and PtIn catalysts are much higher than the one shown by the monometallic catalyst. Taking into account the fact that the cyclohexane dehydrogenation reaction is a facile or structure-insensitive reaction [12], the important increase of the activation energy in PtIn and PtGa with respect to Pt indicates electronic effects of In and Ga on Pt. On the other hand, the Sn effect on Pt would be mainly geometric and not electronic.

Table 1 also shows that the addition of Sn, In and Ga to the Pt catalyst decreases the cyclopentane hydrogenolysis activity, a structure-sensitive reaction carried out on ensembles of active sites [13]. It must be observed that PtIn and PtGa catalysts display lower values of R°_{CH} than the PtSn catalyst.

Table 1 also shows the H_2 chemisorption results for all catalysts. There is a high H_2 chemisorption capacity for the $Pt/MgAl_2O_4$ sample, this value being equivalent to Pt dispersion near 50%. Table 1 shows that the addition of Sn, Ga or In to the Pt catalyst decreases the values of H_2 chemisorption. The Sn addition produces a strong fall of H_2 chemisorption with respect to the Pt catalyst, but this decrease is lower when In or Ga are added to Pt. Taking into account that there are no important modifications in particle size between mono, bi and trimetallic catalysts, as observed by TEM (see below), the effects observed in chemisorption measurements and test reactions results cannot be attributed to an increase of the metallic particle size.

By analyzing the results of Table 1, the decrease of the CP hydrogenolysis rate indicates a geometric effect of dilution of the promoter atoms on Pt atoms, which is higher in PtIn and PtGa catalysts than in the PtSn catalyst. There is also a partial blocking effect of Pt active sites by promoter atoms, as observed in chemisorption results, i.e., the chemisorbed hydrogen is lower in bimetallic catalysts than in the Pt catalyst. This phenomenon is more pronounced in the PtSn catalyst. Besides, the values of activation energies (in CH dehydrogenation) indicate the presence of electronic effects in PtIn and PtGa catalysts, but not in PtSn. This electronic modification of the metallic phase would be responsible for the higher decrease in the R°_{CH} of PtIn and PtGa with respect to PtSn. Considering that in the CH dehydrogenation, the limiting step of this reaction is the benzene desorption [14], it seems clear that the electronic effects of In or Ga on Pt sites causes the fall in the desorption rate of the dehydrogenation product (benzene).

The results corresponding to the conversion of *n*-butane in flow experiments are shown in Figs. 1 and 2. The addition of Sn, Ga and In to Pt increases the *n*-butane conversion along the reaction time. The final conversion of the Pt catalyst is 17%, while PtSn, PtIn and PtGa catalysts show final conversions of 28%, 23% and 19%, respectively. The deactivation parameter (ΔX) along time (see Figs. 1 and 2) was defined as: $\Delta X = 100 \times (X_0 - X_f)/X_0$, where X_0 is the initial conver-

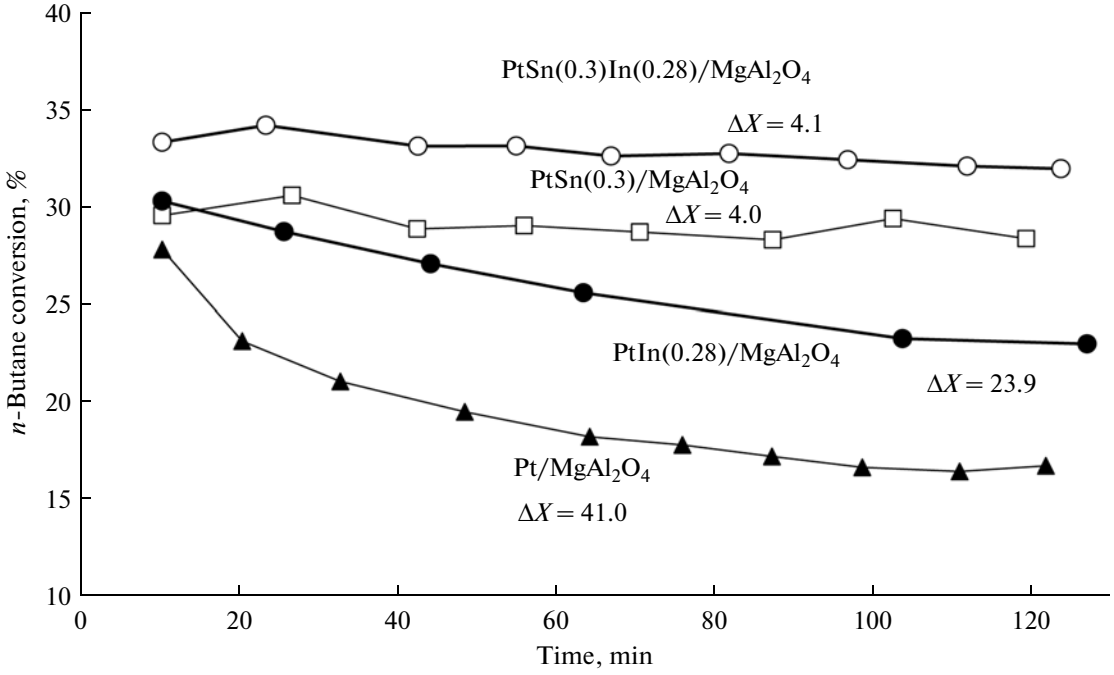

Fig. 1. Values of *n*-butane conversion (*X*) with the reaction time, obtained from flow experiments for Pt, PtSn, PtIn and PtSnIn catalysts supported on $MgAl_2O_4$.

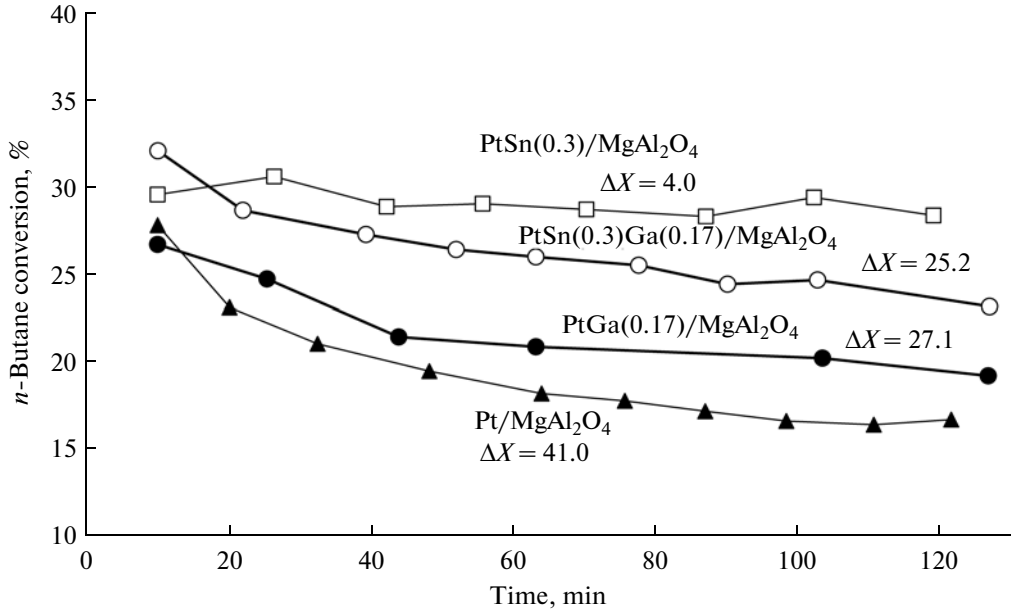

Fig. 2. Values of *n*-butane conversion (*X*) with the reaction time, obtained from flow experiments for Pt, PtSn, PtGa and PtSnGa catalysts supported on $MgAl_2O_4$.

sion (at $t = 10$ min of the reaction time) and X_f is the final conversion (at $t = 120$ min). This deactivation parameter shows high values for the Pt catalyst (41%), and lower values for bimetallic catalysts. In this sense, the PtSn catalyst shows the lowest deactivation parameter (4%), while PtIn and PtGa show intermediate values of 24 and 27%, respectively.

The selectivity to all butenes (1-butene, *cis*- and *trans*-2-butenes, and 1,3 butadiene) in *n*-butane dehydrogenation is shown in Figs. 3 and 4. The addi-

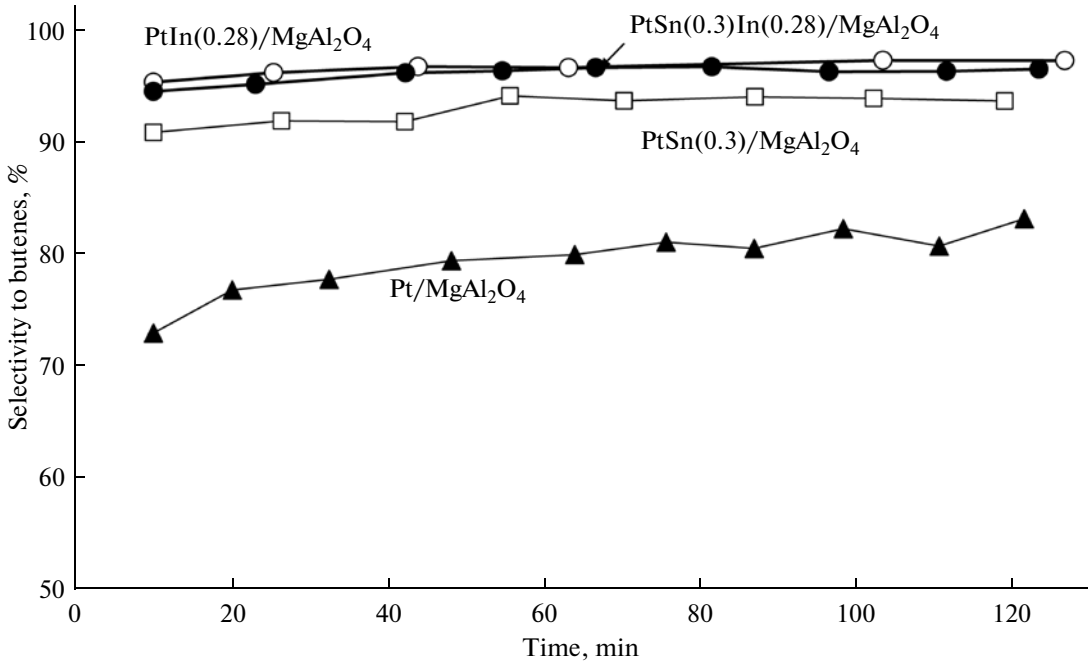

Fig. 3. Selectivity to all butenes (1-butene, *cis*- and *trans*-2-butenes, and 1,3-butadiene) vs. reaction time for Pt, PtSn, PtIn and PtSnIn catalysts supported on $MgAl_2O_4$.

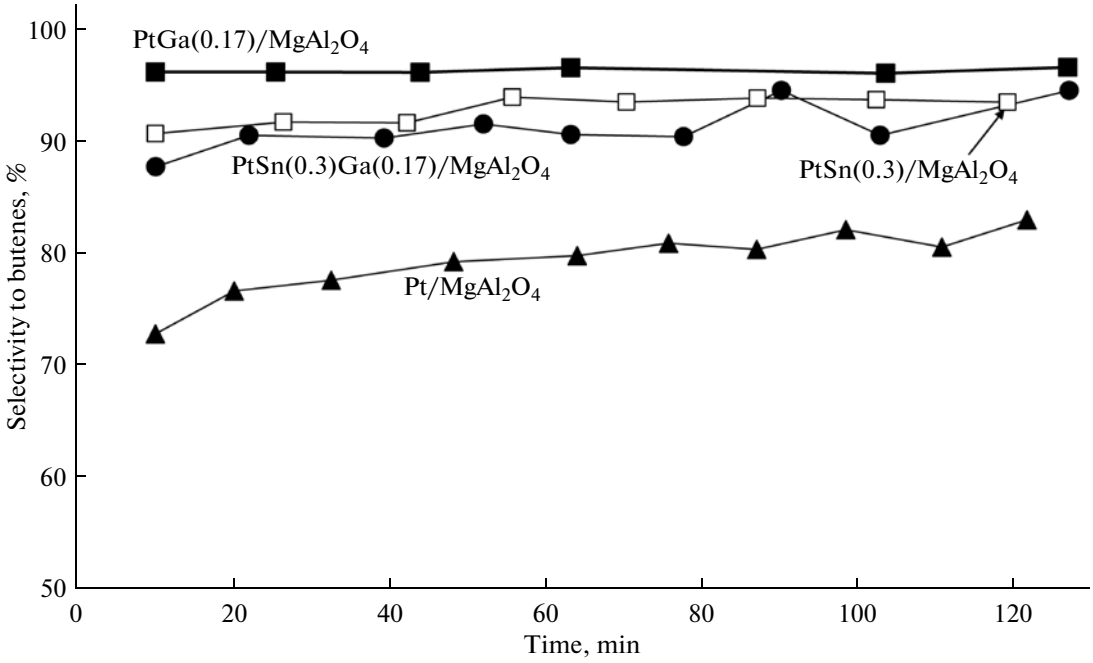

Fig. 4. Selectivity to all butenes (1-butene, *cis*- and *trans*-2-butenes, and 1,3-butadiene) vs. reaction time for Pt, PtSn, PtGa and PtSnGa catalysts supported on $MgAl_2O_4$.

tion of Sn, Ga and In to Pt produces an important increase of the selectivity to butenes along the reaction time. The Pt catalyst shows values from 73% (initial) to 83% (final) in the selectivity to butenes, whereas the bimetallic catalysts show selectivity values higher than 90%. The PtGa and PtIn catalysts show selectivities between 95% and 97%, while the PtSn catalyst displays values from 91% to 94%.

Taking into account the characterization results of bimetallic and monometallic catalysts, the Sn addition to Pt produces mainly geometric effects, strong partial blockage and dilution of Pt atoms. These effects could

Table 2. Results of pulse experiments. Conversion of *n*-butane, selectivity to all butenes and carbon retention (accumulative) for the three first pulses injected to the Pt, PtSn, PtSnIn and PtSnGa catalysts supported on $MgAl_2O_4$

Catalyst	Conversion (%)			Selectivity (%)			C retention (%)		
	pulse number			pulse number			pulse number		
	1	2	3	1	2	3	1	2	3
$Pt/MgAl_2O_4$	94	77	66	1	7	10	35	67	78
$PtSn(0.3)/MgAl_2O_4$	80	73	69	43	58	66	25	35	48
$PtSn(0.3)In(0.28)/MgAl_2O_4$	72	65	59	89	90	90	16	30	43
$PtSn(0.3)Ga(0.17)/MgAl_2O_4$	61	51	40	89	89	89	15	29	40

reduce the undesirable reactions of hydrogenolysis and coke formation, hence increasing the dehydrogenating selectivity to olefins and decreasing the catalyst deactivation, which was also observed by other authors [15,16].

The In and Ga effects on Pt would be of two types: an important dilution of the surface atoms of Pt (geometric effect), which decreases the hydrogenolysis reactions (thus achieving higher selectivities to all butenes than the PtSn catalyst), and electronic effects that would modify the desorption properties of the metallic phase, as observed in CH dehydrogenation results. This effect could favour the formation of coke precursors with high C/H ratio, thus leading to a higher deactivation of PtIn and PtGa catalysts, compared with PtSn.

By comparing the yields to butenes (defined as the product between conversion and selectivity) displayed by the three bimetallic catalysts, the best catalytic performance in *n*-butane dehydrogenation corresponds to the PtSn catalyst, which presents very high and constant yields to butenes (from 26.9% to 26.6%). On the other hand, there is a decrease of the yield to butenes both in PtIn (from 28.9% to 22.4%) and in PtGa (from 25.7 to 18.6%).

Influence of In and Ga Addition to $PtSn/MgAl_2O_4$ Catalysts. Evaluation of Trimetallic Catalysts in n-Butane Dehydrogenation

Once Sn is selected as the second metal added to Pt, the effect of adding a third metal, like In or Ga, was subsequently studied.

Figures 1 and 2 also show the values of the *n*-butane conversion (X) with the reaction time, obtained from flow experiments for trimetallic catalysts supported on $MgAl_2O_4$. It can be observed that the addition of In or Ga to PtSn produces changes in the catalytic behavior. Both trimetallic catalysts have an initial conversion of 32–33%, which was slightly higher than that of the PtSn sample (30%). However, while the PtSnIn catalyst was very stable ($\Delta X = 4.1\%$), the PtSnGa deactivated during the reaction ($\Delta X = 25.2\%$).

Figures 3 and 4 also show the values of the selectivity to all butenes for trimetallic catalysts supported on $MgAl_2O_4$. For PtSn and PtSnGa catalysts, the selectivity is similar and it ranges from 88 to 93%, and for PtSnIn the selectivity is the highest with constant values at about 95–96%.

In conclusion, results of *n*-butane dehydrogenation indicate that the addition of Ga to the bimetallic catalyst does not improve the dehydrogenation performance, while the addition of In produces an increase in both the activity and selectivity to butenes, and maintains the low value of the deactivation parameter.

Pulse experiments were carried out to study the initial steps of the *n*-butane dehydrogenation reaction, which cannot be observed in flow experiments. Three pulses of pure *n*-butane were injected on each sample during the pulse experiments. Results of the *n*-butane conversion (X), selectivity to all butenes and carbon retention as a function of the pulse numbers are indicated in Table 2. It can be observed that the monometallic catalyst displays higher *n*-butane conversion after the injection of the first pulse than bi and trimetallic ones. However, the initial activity of the monometallic catalysts in flow experiments (see Figs. 1 and 2) is lower than those of bi and trimetallic ones. The higher initial activity for PtSn, PtSnGa and PtSnIn catalysts observed in flow experiments with respect to the monometallic one can be explained by considering the results of carbon retention obtained in pulse experiments. In Table 2 it can be observed that the carbon retentions after the injection of the first pulses of *n*-butane for monometallic catalysts are clearly higher than for the bimetallic and trimetallic ones. It should be considered that the injection of the first pulse of *n*-butane is produced on a clean surface (carbon free), in contrast to the flow experiments, where the initial activity (taken at 10 min of the reaction time) corresponds to the reaction of *n*-butane on a partially deactivated surface by carbon deposition. Hence, taking into account the carbon retention values shown in Table 2, it is observed that the deactivation by coke deposition is very important for monometallic catalysts, thus producing a strong decrease of the activity during the initial steps of the reaction.

With respect to the selectivity to all butenes in pulse experiments, Table 2 shows that the values slowly

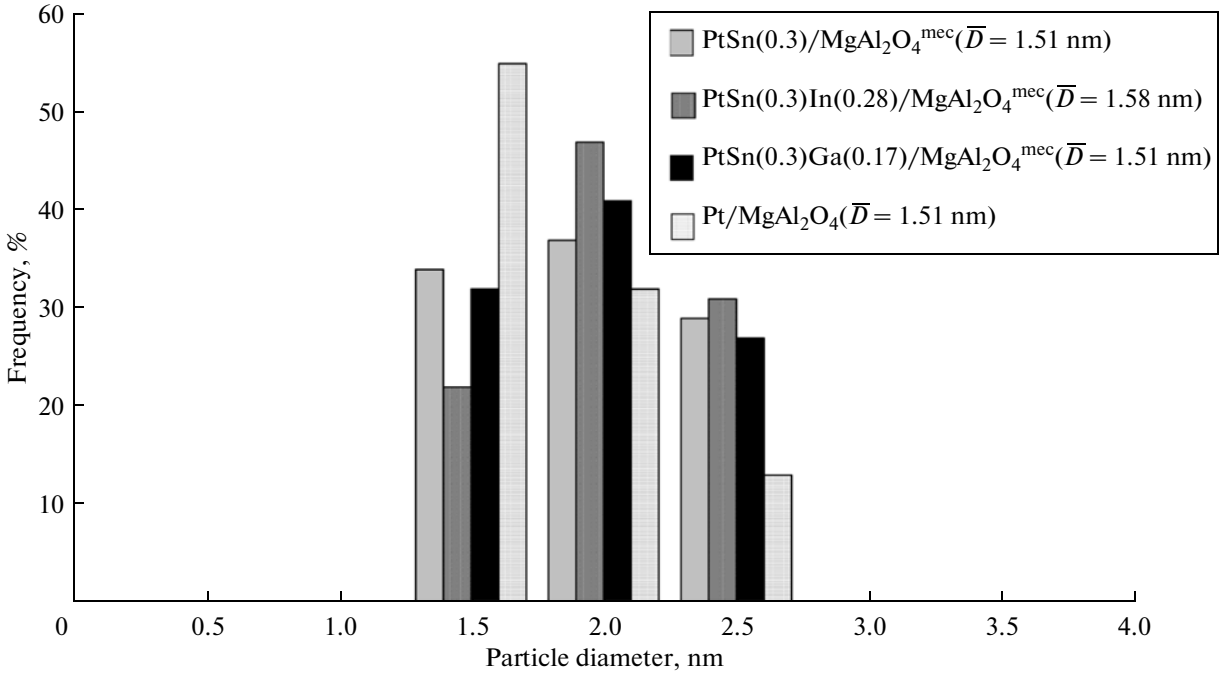

Fig. 5. Distribution of metallic particle sizes by TEM for the different fresh catalysts.

increase as the pulse number increases for mono and bimetallic catalysts, but it remains unchanged for both trimetallic samples. It can be observed that the selectivity to olefins on the $Pt/MgAl_2O_4$ catalyst after the first pulse is only 1%, while that corresponding to the PtSn catalyst is much higher (43%), and those corresponding to trimetallic catalysts are very high (≅90%). This latter value, which remained practically constant along the three pulses, is similar to that observed in flow experiments for both trimetallic catalysts. On the other hand the selectivity values for the three pulses in mono and bimetallic catalysts are much lower than the ones obtained in flow experiments (see Figs. 3 and 4). In mono and bimetallic catalysts, there is a clear correlation between the carbon retention and the evolution of the selectivity to butenes along the pulses, which indicates that both fresh catalysts (mainly the monometallic one) have an important concentration of hydrogenolytic sites that are blocked by carbon during the first steps of the reaction, thus increasing the dehydrogenating selectivity. On the other hand, in the metallic phase of both trimetallic catalysts, there is a very low concentration of hydrogenolytic sites since the selectivity to olefins is very high in the initial steps of the reaction and it remains unchanged along the reaction time.

Characterization of the Metallic Phase of Trimetallic Catalysts

Experiments of cyclohexane (CH) dehydrogenation were also carried out on trimetallic catalysts, and the results are shown in Table 1. For trimetallic PtSnGa and PtSnIn catalysts, a pronounced decrease of the CH dehydrogenation reaction rate with respect to the bimetallic PtSn catalyst is observed in Table 1. Precise measurements of the activation energy for trimetallic catalysts could not be determined due to the very low activity in this reaction.

Results of the cyclopentane hydrogenolysis are also indicated in Table 1. The CPH activity decreases after the addition of Sn to the $Pt/MgAl_2O_4$ catalyst, and the decrease is more important after the addition of the third metal (In or Ga) to Pt.

Table 1 also shows the values of the chemisorbed hydrogen on trimetallic catalysts supported on $MgAl_2O_4$. When Sn is added to Pt, the H_2 chemisorption capacity decreases three times, while for both trimetallic catalysts, the H_2 chemisorption is negligible.

TEM results displayed in Fig. 5 indicate that there are no important changes in the distribution of metallic particle size after addition of Sn, In or Ga to the Pt catalyst, since the mean diameters are 1.32 nm, 1.51 nm, 1.51 nm and 1.58 nm for Pt, PtSn, PtSnGa and PtSnIn, respectively.

Taking into account TEM results (similar particle size in mono-, bi-, and trimetallic catalysts), the important decrease of the chemisorption values for trimetallic catalysts, together with the negligible activity in CH dehydrogenation and the very low hydrogenolytic activity could be attributed to different geometric effects of Sn, In or Ga on Pt sites, like blocking and dilution, though the presence of electronic effects should not be discarded (as observed for PtIn and PtGa catalysts).

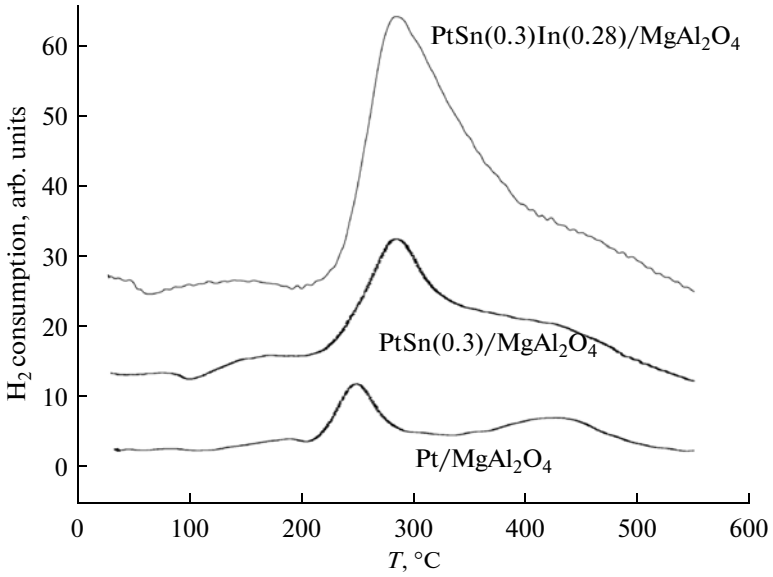

Fig. 6. TPR profiles of calcined Pt, PtSn and PtSnIn catalysts supported on $MgAl_2O_4$.

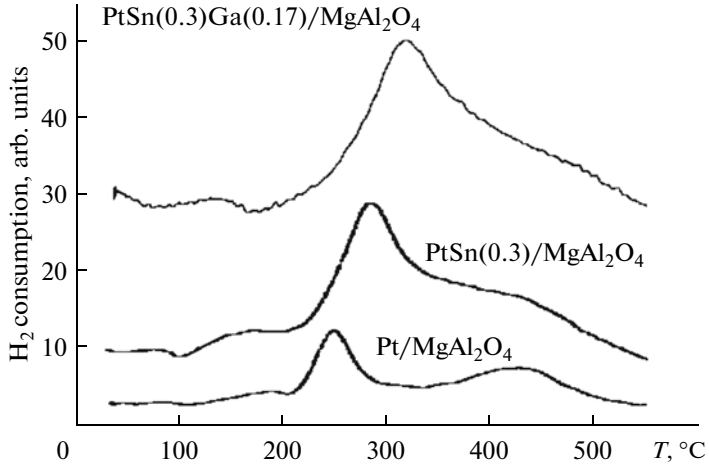

Fig. 7. TPR profiles of calcined Pt, PtSn and PtSnGa catalysts supported on $MgAl_2O_4$.

Figures 6 and 7 show the TPR profiles of mono, bi and trimetallic catalysts. The reduction profile of the Pt catalyst shows two peaks, the main one at 235°C and the second one, smaller and wider, at 410°C. These peaks would correspond to the reduction of different Pt oxichlorinated species [17]. In the bimetallic PtSn catalyst, the addition of Sn to Pt produces both a broadening and a shift of the main reduction peak toward higher temperatures (275°C) (Figs. 6 and 7). This fact indicates the Pt–Sn coreduction. In addition to this main peak, the PtSn catalyst shows a shoulder at higher temperatures (between 390 and 480°C) probably attributed to the reduction of free Sn species since in the $Sn/MgAl_2O_4$ catalyst, a reduction zone at high temperature (>400°C) was also observed. TPR profiles of PtSnIn (Fig. 6) and PtSnGa catalysts (Fig. 7) display broad and high reduction peaks which are shifted to much higher temperatures (290 and 300°C, respectively). In conclusion, the bigger size of the main peak observed in bimetallic and trimetallic systems together with the shift to higher temperatures and the broadening of this peak after the addition of Sn and In or Ga to Pt could be related to either a catalytic effect of Pt on the metallic promoters reduction (the hydrogen dissociated on Pt particles would reduce Sn and In or Ga) or a simultaneous reduction of the metals with probable alloy formation. These results are in agreement with characterization results presented in Table 1.

Table 3 shows the binding energy (BE) values corresponding to the Sn $3d_{5/2}$ level of $PtSn/MgAl_2O_4$, $PtSnIn/MgAl_2O_4$ and $PtSnGa/MgAl_2O_4$ catalysts

Table 3. XPS results for PtSn, PtSnIn and PtSnGa catalysts supported on $MgAl_2O_4$ (The values between parentheses correspond to the percentage of each species)

Catalyst	Binding energy $Sn3d_{5/2}$ (eV)	Binding energy M* (eV)
$PtSn/MgAl_2O_4$	483.1 (16%) 486.1 (69%) 487.4 (15%)	–
$PtSn(0.3)In(0.28)/MgAl_2O_4$	483.2 (35%) 486.4 (58%) 487.7 (7%)	444.3 (64%) 445.8 (36%)
$PtSn(0.3)Ga(0.17)/MgAl_2O_4$	483.4 (26%) 486.6 (71%) 488.5 (3%)	22.4(100%)

* Corresponding to In $3d_{5/2}$ or Ga 3*d*.

after reduction in situ at 500°C. From the deconvolution of the $Sn3d_{5/2}$ spectra of the three catalysts, three peaks were obtained at 483.1–483.4 eV, 486.1–486.6 eV and 487.4–488.5 eV. It can be observed that the first peak corresponds to a fraction of Sn in the zerovalent state (16% in PtSn, 35% in PtSnIn and 26% in PtSnGa catalysts). The other two peaks are attributed to different oxidized and oxychlorinated species of Sn stabilized on the support [18,19]. The presence of Sn(0) in bimetallic and trimetallic catalysts and the absence of this species in the Sn monometallic one [20], would indicate a higher Sn reducibility in PtSn, PtSnIn and PtSnGa catalysts, these results agreeing with TPR ones.

Besides, Table 4 also shows the binding energy values corresponding to In $3d_{5/2}$ in $PtSnIn/MgAl_2O_4$ and to Ga3*d* level in $PtSnGa/MgAl_2O_4$ catalysts after reduction in situ at 500°C. For the PtSnIn sample, two signals could be deconvoluted, the former at 444.3 eV corresponding to zerovalent In (64% of the total surface In), and the latter at 445.8 eV corresponding to oxidized In (36% of the total surface In) [19]. For the PtSnGa sample, only one signal was observed at 22.4 eV corresponding to oxidized Ga. Hence, a higher reducibility of In than that of Ga in the corresponding trimetallic catalysts is observed. This is in agreement with the work of Homs et al. [18] who studied $PtSnM/SiO_2$ catalysts (M = Ga, In, Tl) by XPS.

Studies on the Stability of Mono-, Bi-, and Trimetallic Catalysts

The stability experiments were carried out through five successive reaction-regeneration cycles, which were described in the experimental section, and the results are condensed in Table 4. It shows the modification of the initial and final yield to butenes (defined as the product between the *n*-butane conversion and the selectivity to all butenes) for $MgAl_2O_4$ supported Pt (taken as a reference), PtSn, PtSnGa and PtSnIn catalysts, through the successive reaction-regeneration cycles. It can be observed that the monometallic catalyst showed a pronounced decrease of the yield to butenes in each cycle and along the five cycles. In this sense the fall in the yield (ΔY) between the initial yield of the first cycle and the final yield of the last cycle, referred to initial yield of the first cycle, was 57%. The yields to butenes for the $PtSn/MgAl_2O_4$ and $PtSnGa/MgAl_2O_4$ catalysts are slightly modified through the successive cycles, and the ΔY values for both catalysts are 16% and 14%, respectively. However, the ΔY value of $PtSnIn/MgAl_2O_4$ remains constant, thus showing an excellent stability along the cycles. In order to obtain a better comparison of the performance along the cycles of the different catalysts, the yields to butenes as a function of the reaction time during the last cycle (after four reaction periods and four regeneration steps) are shown in Fig. 8. The trimetallic $PtSnIn/MgAl_2O_4$ catalyst clearly displayed the best stability, thus showing in the last cycle a slight decrease of the yield from 32 to 29%. In spite of the lower stability of PtSnGa and the bimetallic PtSn sample with respect to that corresponding to the PtSnIn

Table 4. Values of initial yield (Y_0) and final yield (Y_f) for $MgAl_2O_4$-supported Pt (taken as a reference), PtSn, PtSnGa and PtSnIn catalysts, through the five successive reaction-regeneration cycles

Catalyst	Cycle 1		Cycle 2		Cycle 3		Cycle 4		Cycle 5	
	Y_0	Y_f	Y_0	Y_f	Y_0	Y_f	Y_0	Y_f	Y_0	Y_f
$Pt/MgAl_2O_4$	30	18	26	15	26	14	25	13	25	13
$PtSn/MgAl_2O_4$	31	26	33	25	30	25	32	25	29	26
$PtSnGa/MgAl_2O_4$	29	25	34	28	35	30	33	26	34	25
$PtSnIn/MgAl_2O_4$	28	25	34	30	32	30	33	32	32	29

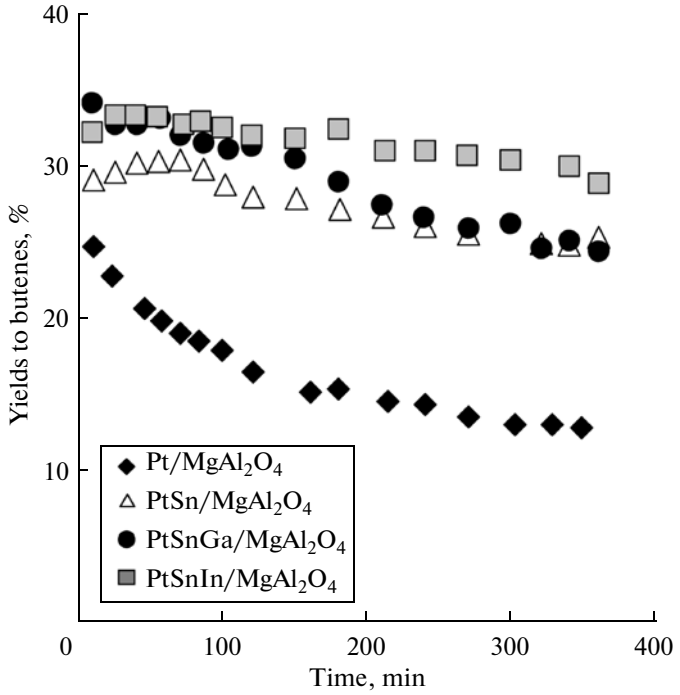

Fig. 8. Yields to butenes of the different catalysts as a function of the reaction time during the last reaction-regeneration cycle (after four reaction periods and four regeneration steps).

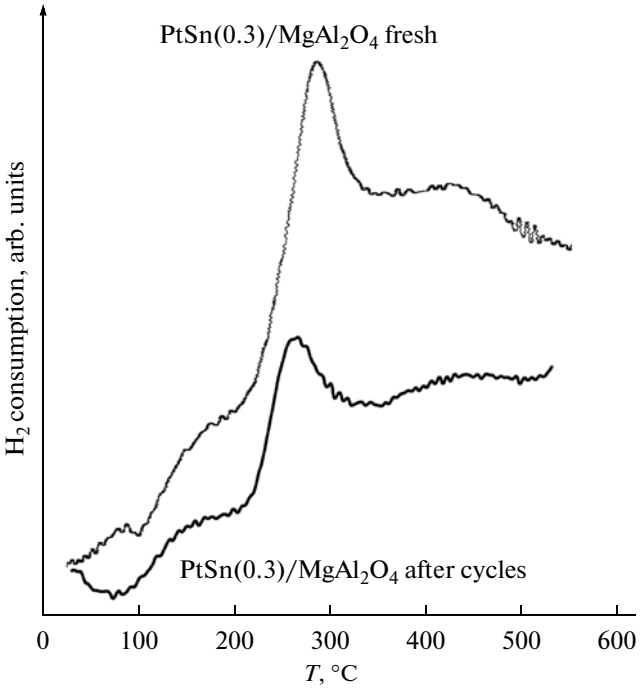

Fig. 9. TPR profiles of fresh and after cycles $PtSn/MgAl_2O_4$ catalysts.

catalyst, they also showed a very good behavior through the successive reaction-regeneration cycles.

In general, the modification of the structure of the metallic phase would take place from cycle to cycle. Each cycle involves the reaction step, the burning of the deposited coke (exothermic reaction) and the reduction of the metal (exothermic process). All these effects can lead to the modification of the metallic phase, though in a different degree according to the nature of the support, the characteristics of the active phase related to the promoters added to the active metal. Figures 9, 10 and 11 show the TPR profiles of the bimetallic PtSn and trimetallic PtSnGa and PtSnIn catalysts, both fresh and after reaction-regeneration cycles. In all cases, the TPR profiles corresponding to catalysts after the five reaction-regeneration cycles show that the shape and the temperatures of the reduction peaks are very similar to those of the fresh samples, though these peaks have minor areas. This means that the metallic phases of these catalysts are modified in a low extension after the cycles. These results agree with those obtained by TEM of the samples after cycles, which indicate that the metallic particle size of PtSn (mean diameter = 1.42 nm) and PtSnIn catalysts (mean diameter = 1.40 nm) did not increase after the five cycles. The results of these tests show that the metallic phases of these catalysts are very stable and resistant to sintering processes.

On the other hand, in the monometallic $Pt/MgAl_2O_4$ catalyst submitted to the successive reaction-regeneration cycles, the narrow TPR reduction zone appearing at 235°C (Fig. 12) displayed by the fresh sample, becomes broader and shifted to lower temperatures in the TPR of the catalyst after cycles. This new peak at 190°C would correspond to the reduction of metallic particles with higher size, origi-

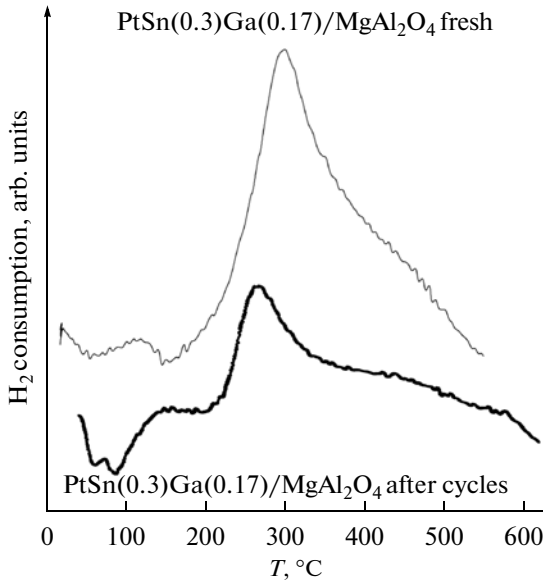

Fig. 10. TPR profiles of fresh and after cycles $PtSnGa/MgAl_2O_4$ catalysts.

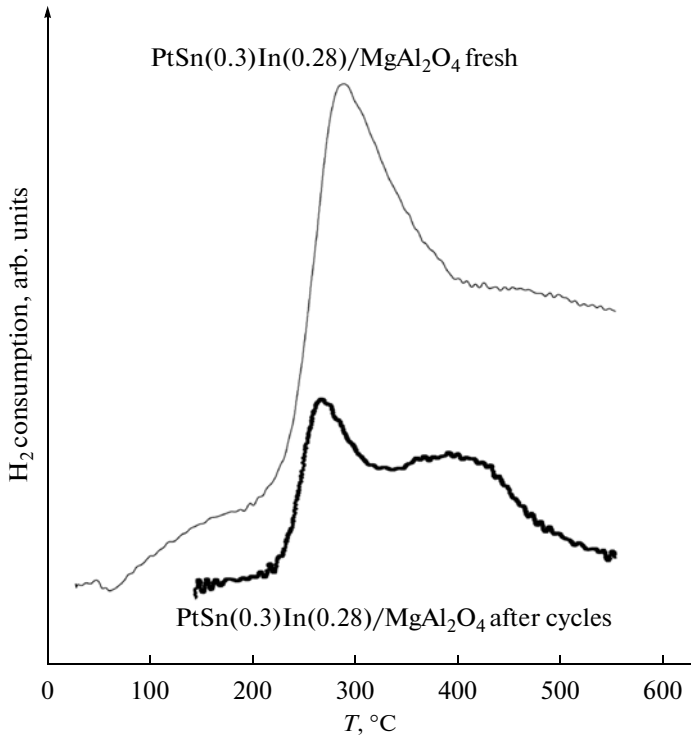

Fig. 11. TPR profiles of fresh and after cycles $PtSnIn/MgAl_2O_4$ catalysts.

nated during the cycles. This important modification of the metallic phase in the $Pt/MgAl_2O_4$ catalyst along the cycles is responsible for the low catalytic stability of the monometallic catalyst.

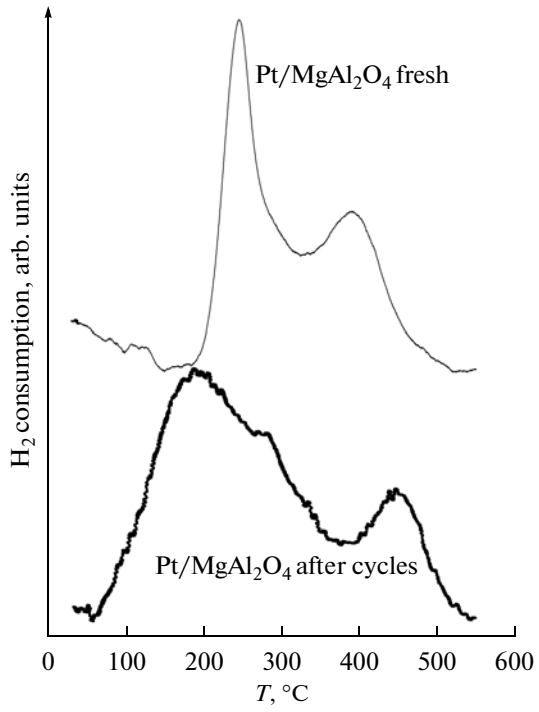

Fig. 12. TPR profiles of fresh and after cycles $Pt/MgAl_2O_4$ catalysts.

CONCLUSIONS

Results of *n*-butane dehydrogenation corresponding to bimetallic catalysts showed that the PtSn catalyst has a better catalytic behavior than PtIn and PtGa ones. The characterization results indicate the presence of geometric effects for the former catalyst, and geometric and electronic effects for PtIn and PtGa.

For trimetallic catalysts, while the addition of Ga to the bimetallic catalyst does not practically modify the dehydrogenation performance, the addition of In produces an increase both of the activity and the selectivity to butenes.

Pulse reactions results displayed that both Pt and PtSn fresh catalysts (mainly the monometallic one) have an important number of hydrogenolytic sites that are blocked by carbon during the initial steps of the reaction. On the other hand, in the metallic phase of both trimetallic catalysts, very low concentrations of hydrogenolytic sites are present.

Taking into account that there are no important changes in metallic particle size after the addition of Sn, In or Ga to the Pt catalyst, as observed by TEM, characterization results clearly indicate the presence of a close contact between Pt, Sn and In or Ga in both trimetallic catalysts. The geometric effects, like blocking and dilution of the active sites by the promoters, are present in

these catalysts, though the electronic effects could also play a role in both trimetallic catalysts.

The trimetallic $PtSnIn/MgAl_2O_4$ catalyst clearly displayed the best catalytic stability during experiments of reaction-regeneration cycles. In spite of the lower stability of PtSnGa and PtSn catalysts with respect to $PtSnIn/MgAl_2O_4$, they also showed a very good behavior through the successive cycles. The characterization of these catalysts by TPR and TEM showed that the metallic phase of bi and trimetallic catalysts remains practically unmodified along the cycles.

ACKNOWLEDGMENTS

The authors thank the Secretaría de Ciencia y Técnica- Universidad Nacional del Litoral (CAI+D Program) and ANPCYT for the financial support of this Project. Thanks are also given to Miguel A. Torres for the experimental assistance.

REFERENCES

1. Bhasin, M., McCain, J., Vora, B., Imai, T., and Pujadó, P., *Appl. Catal. A*, 2001, vol. 221, p. 397.
2. Siddiqi, G., Sun, P., Galvita, V., and Bell, A., *J. Catal.,* 2010, vol. 274, p. 200.
3. Bocanegra, S., de Miguel, S., Castro, A., and Scelza, O., *Catal. Lett.*, 2004, vol. 96, p. 129.
4. Armendáriz, H., Guzmán, A., Toledo, J., Llanos, M., Vazquez, A., and Aguilar-Ríos, G., *Appl. Catal. A*, 2001, vol. 211, p. 69.
5. Siri, G., Ramallo-López, J., Casella, M., Fierro, J., Requejo, F., and Ferretti, O., *Appl. Catal. A*, 2005, vol. 278, p. 239.
6. Llorca, J., Ramírez de la Piscina, P., León, J., Sales, J., Fierro, J., and Homs, N., *Stud. Surf. Sci. Catal.*, 2000, vol. 130, p. 2513.
7. Ballarini, A., Zgolicz, P., Vilella, I., de Miguel, S., Castro, A., and Scelza, O., *Appl. Catal. A,* 2010, vol. 381, p. 83.
8. Rennard, R. and Freel, J., *J. Catal.*, 1986, vol. 98, p. 235.
9. Bocanegra, S., Zgolicz, P., Scelza, O., and de Miguel, S., *Catal. Commun.*, 2009, vol. 10, p. 1463.
10. Domansky, D., Urretavizcaya, G., Castro, F., and Gennari, F., *J. Am. Ceram. Soc.,* 2004, vol. 87, p. 2020.
11. Bocanegra, S., Ballarini, A., Scelza, O., and de Miguel, S., *Mater. Chem. Phys.*, 2008, vol. 111, p. 534.
12. Rodríguez-Ramos, I. and Guerrero-Ruiz, A., *Journal of Catalysis,* 1992, vol. 135, p. 458.
13. Borgna, A., Garetto, T., and Monzón, A., *J. Chem. Soc., Faraday Trans.*, 1997, vol. 93, p. 2445.
14. Koel, B., Blank, D., and Carter, E., *J. Mol. Catal. A,* 1998, vol. 131, p. 39.
15. Cortright, R. and Dumesic, J., *J. Catal.*, 1994, vol. 148, p. 771.
16. Passos, F., Aranda, D., and Schmal, M., *J. Catal.*, 1998, vol. 178, p. 478.
17. Mazzieri, V.A., Grau, J.M., Vera, C.R., Yori, J.C., Parera, J.M., and Pieck, C.L., *Catal. Today*, 2005, vol. 107, p. 643.
18. Homs, N., Llorca, J., Riera, M., Jolis, J., Fierro, J., Sales, J., and Ramírez de la Piscina, P., *J. Mol. Catal. A: Chem.*, 2003, vol. 200, p. 251.
19. Moulder, J.F., Stickle, W.F., Sobol, P.E., and Bomben, K., *Handbook of X-ray Photoelectron Spectroscopy*, 2nd ed., Chastain, J., Ed., Perkin-Elmer Corporation (Physical Electronics), 1992.
20. Bocanegra, S., Guerrero-Ruíz, A., de Miguel, S., and Scelza, O., *Appl. Catal. A*, 2004, vol. 277, p. 11.